Nigerian Journal of Engineering
Faculty of Engineering
Ahmadu Bello University
Samaru - Zaria, Nigeria

Vol. 26, No. 3, December 2019
ISSN: 0794 - 4756

EFFECT OF SWIRL ON THE COMBUSTION AND EMISSION CHARACTERISTICS OF HYDROGEN ENRICHED METHANE IN A MODEL GAS TURBINE COMBUSTOR

Y. S. Sanusi and H. A. Dandajeh

Department of Mechanical Engineering, Ahmadu Bello University, Zaria, Nigeria
Corresponding Author's Email: syssanusi@abu.edu.ng

ABSTRACT

Modifications in the existing power plants in reducing emissions of carbon monoxide (CO) and nitrogen oxides (NOx)is central to global reduction of pollutant emissions. Varying the swirl number (SN) of the combustor inflow can be used to modify the dynamics of the combustion and emissions. This paper presents numerical investigation into the effect of swirl number on the combustion and emission characteristics in a gas turbine model combustor. Flame with swirl numbers of 0.38, 0.67 and 1.15 were studied using hydrogen enriched flame. A modified two step global chemical reaction mechanism with 1-step global mechanism of hydrogen by Marinov was used to model the combustion of hydrogen enriched methane. The discrete ordinates (DO) radiation model with Weighted Sum of Gray Gases model (WSGGM) was used to account for the radiation heat loss between the combustion gases and combustion chamber wall. The developed model predicted the temperature profile and emissions within 10% of the experimental values. Results further show that flames with SN of 0.67 have the highest size and strength of the recirculation zone that enhance flame stabilization as compared to flames with othe r swirl numbers. The NOx emission was observed to decrease with increasing SN at all operating conditions. This was due to the decreased combustion maximum temperature as the SN increases. However, the dynamics of the CO emission depends on the fuel composition. For instance, pure methane (0% H_2), flames with SN of 0.67 gave the minimum CO emission, while, the CO emission decreased with increasing SN when methane and hydrogen composition in the fuel mixture were of the same order. The decreased CO emission was due to improved mixing and higher flame temperature in the combustor that aid the complete combustion of CO to CO_2.

Keywords: *NOx emissions; CO emissions; hydrogen-enriched methane; Swirl number; swirl stabilized combustor*.

INTRODUCTION

There are stringent global regulations on pollutant emissions such as CO and NOx (Mokheimer *et al*., 2015). In January 2010, United State Environmental Protection Agency (USEPA) established an additional primary standard at 100 ppb, averaged over one hour for NOx emission (USEPA 2015). More recently, California adopted best available control technology (BACT) standards limiting NOx emissions from new simple-cycle gas turbine plants to 5 ppm, and for new combined cycles, 2.5 ppm (USEPA 2018). Experts in the power generation industry are adopting new measures to meet the stringent regulations of pollutant gas emissions in the design of new power plants. However, there are concerns on the type of modifications to be carried out in the existing plants that operate outside the regulated emission window. These modifications are to be carried out so as to have minimal effect on the plant performance. Retrofitting of power plant to meet the required pollutant emissions standard has proved beneficial. For instance, Chevron's Eastridge Cogeneration Plant, California has been retrofitted to meet San Joaquin Valley Rule 4703 requiring reduction of the current 42 ppm NOx emissions to 12 ppm (~70 % reduction) with annual cost saving from NOx reduction of about $0.5-million per year(Seebold *et al*., 2001). Retrofitting can also be done by controlling the combustion to reducing NOx emissions in gas turbines and boilers. This can be achieved by controlling the flow pattern in to the combustion chamber so as to control the mixing of the fresh charge with the combustion product and vary the residence time of the combustion product. Swirling flow has been reported to: (1) improve mixing and provide better flame stabilization in a combustor, (2) provide aerodynamic stability to the combustion process by producing regions RZ and (3) increase residence time of the reactants in the FZ thus improving the combustion efficiency (Liu *et al*., 2017). Several experimental and numerical studies have been carried out in a swirl stabilized combustor (Mokheimer *et al*., 2015; Sanusi *et al*., 2015; Shanbhogue *et al*., 2016; Li *et al*., 2008; Weigand *et al*., 2006; Sanusi *et al*., 2017; Nemitallah and Habib 2013). Mokheimer *et al*. (2015) numerically studied combustion characteristics in swirl combustor, while, Sanusi *et al*. (2015) studied the flame stability and emission characteristics in a swirl combustor. Sanusi *et al*. (2017) and Nemitallah and Habib (2013) carried out experimental studies on oxy-flame characteristics in a swirl combustor. Shanbhogue *et al*. (2016) and Li *et al*. (2008) however, focused on the flow- flame interactions and flame stabilization with little attention given to the effect of swirl on emissions. Consequently this work is aimed at investigating the role of swirl on the combustion and emission characteristics in a gas turbine model combustor. The study was carried out numerically using computational fluid dynamics (CFD) approach. The approach has become popular in recent years due to its lower cost compared to experimental studies (Habib *et al*., 2014). Experiments were first carried out in a swirl stabilized combustor at a swirl number of 0.67 and different operating conditions (i.e. 0% H_2, Ø=0.5: 50% H_2, Ø=0.5: 50% H_2, Ø=0.3). Numerical code was then developed using appropriate mathematical models (i.e., chemistry, radiation, and turbulence models). The models were then validated with experimental observed values. The validated models were thereafter used to study hydrogen enriched flame having swirl numbers of 0.38, 0.67

and 1.15.Swirl numbers of 0.38, 0.67 and 1.15 is equivalent to swirl angle of 30°, 45°, and 60° respectively. It is important to state that swirl number is the ratio of the momentum of the tangential flow component to that of the axial flow component. All analysis in this work was carried out under atmospheric condition.

Mathematical modeling

The mathematical equations describing fuel oxidation and flow in the model combustor were based on the conservation equations of mass, momentum, species and energy as well as equations for turbulence and radiation. The generalized equation that governs the conservation of mass, momentum and energy as well as the equations for species transport can be written as (Reynolds 1987.; Shih *et al*., 1995; Habib *et al*.,):

$$\frac{\partial}{\partial x_j}\left(\bar{\rho}\bar{u}_j\emptyset + \bar{\rho}\overline{u_j'\emptyset'}\right) = \frac{\partial}{\partial X_j}\left(\Gamma_{\emptyset}\frac{\partial\emptyset}{\partial x_j}\right) + \bar{\rho}S_{\emptyset} \quad (1)$$

From Equation (1), the continuity Equation is given as:

$$\frac{\partial}{\partial x_j}\left(\bar{\rho}\bar{u}_j\right) = 0 \quad (2)$$

The momentum equation is given as:

$$\frac{\partial\left(\overline{\rho u_i u_j}\right)}{\partial x_j} = -\frac{\partial\bar{P}}{\partial x_i} + \frac{\partial\left(\bar{t}_{ij}+\bar{\tau}_{ij}\right)}{\partial x_j} \quad (3)$$

where, $\bar{t}_{ij}$ is the viscous stress tensor given in Equation (4) (Ghenai 2010):

$$\bar{t}_{ij} = \mu\left[\left(\frac{\partial\overline{u_i}}{\partial x_j}+\frac{\partial\overline{u_j}}{\partial x_i}\right) - \frac{2}{3}\frac{\partial\overline{u_k}}{\partial x_k}\delta_{ij}\right] \quad (4)$$

$$\delta_{ij} = 1 \; if \; i = j, \delta_{ij} = 0 \; if \; i \neq j$$

The average Reynolds stress tensor is defined as (Ghenai 2010):

$$\bar{\tau}_{ij} = -\overline{\rho u_i' u_j'} \quad (5)$$

$$\bar{\tau}_{ij} = \mu_t\left[\left(\frac{\partial\overline{u_i}}{\partial x_j}+\frac{\partial\overline{u_j}}{\partial x_i}\right) - \frac{2}{3}\frac{\partial\overline{u_k}}{\partial x_k}\delta_{ij}\right] - \frac{2}{3}\left(\overline{\rho k\delta_{ij}}\right) \quad (6)$$

The RNG-based k-ε turbulence model was used in this work. The RNG $k-\varepsilon$ model (Yakhot and Orszag 1986; Smith and Woodruff 1998)has an additional term in its turbulent dissipation equation that significantly improves the accuracy for rapidly strained flow. It also accounts for the effect of swirl on turbulence, thus, enhancing the accuracy of swirling flow. To account for the effect of swirl or rotation, the turbulence viscosity is calculated as:

$$\boldsymbol{\mu_t = \mu_{t0}\, f\left(\alpha_s, \cap, \frac{k}{\varepsilon}\right)} \quad (7)$$

where, μ_{t0} is the turbulent viscosity calculated without the swirl modification and given in Equation (8):

$$\boldsymbol{\mu_{t0} = \rho C_\mu \frac{k^2}{\varepsilon}} \quad (8)$$

$\cap$ is the characteristics swirl number while α_s is the swirl constant set as 0.07.

The model constants have the following values:

$$C_\mu = 0.0845\,, C_{1\varepsilon} = 1.42,\;\; C_{2\varepsilon} = 1.68$$

For the purpose of the near wall treatment, the standard wall function was used in this work to couple the field variables and the corresponding cell variables near the wall.

Energy Equations

The energy equation was solved to account for heat transfer due to conduction, species diffusion, viscous dissipation as well as energy source terms (Ghenai 2010) as given in Equation (9).

$$\frac{\partial}{\partial x_j}\overline{(\rho E + P)u_j} = \frac{\partial}{\partial x_j}\left(K_{eff}\left(\frac{\partial\bar{T}}{\partial x_j}\right) - \sum_j h_j J_j + \tau_{eff}u_j\right) + S_h \quad (9)$$

$$E = h - \frac{P}{\rho} + \frac{v^2}{2} \quad (10)$$

where, k_{eff} is the effective conductivity calculated using Equation (11).

$$K_{eff} = k + k_t \quad (11)$$

S_h is the energy source term that includes the reaction source term and radiation heat exchange.

Radiation model

The radiative transfer equation (RTE) was solved using the discrete ordinates (DO) radiation model as given inref. (Nemitallah and Habib). This was to obtain the radiation heat exchange between the wall and combustion gases.

$$\frac{dI(r,s)}{ds} = kI_b - (k+\sigma_s)I(r,s) \quad (12)$$

$$k(T,P) = \frac{\int k_\lambda(\lambda,T,P)e_{b\lambda}(\lambda,T)d\lambda}{\sigma T^4} \quad (13)$$

The variables given by (Zheng *et al*., 2000)is used to compute the blackbody spectral emissive power. The Weighted Sum of Gray Gases model (WSGGM) which is dependent on gas composition and temperature was used to properly account for the radiation heat exchange between gases and the combustion chamber wall.

Species transport model

The solution of a convection–diffusion equation for the l^{th} species is shown in Equation (14). This equation can be used to predict the mass fraction of species Y_l .

$$\frac{\partial}{\partial x_i}(\rho\bar{u}_i Y_l) = -\frac{\partial}{\partial x_i}Y_{l,i} + R_l \quad (14)$$

The species source term R_l is the net rate of production or consumption of species l by chemical reaction while $D_{l,i}$is the diffusion flux of species $l$as shown in Equation (15).

$$Y_{l,i} = -\left(\rho D_{l,i} + \frac{\mu_t}{SC_t}\right)\frac{\partial Y_l}{\partial x_i} \quad (15)$$

Sc_t is the turbulent Schmidt number and was taken as 0.7.

Reaction Mechanism

Methane combustion was modeled in the present work using a modified two step global chemical reaction mechanism given in (Mokheimer *et al*., 2015). Details of the reaction mechanisms and their Arrhenius constants are summarized in Table 1. In modeling the oxidation of hydrogen enriched methane, the 1-step global mechanism of hydrogen by Marinov *et al*. (Marinov *et al*., 1996) (see Table 2) was incorporated with the global reaction mechanisms of methane given in Table 1. The obtained equations were used to model the combustion of hydrogen enriched methane. (De and Acharya 2012) similarly incorporated H_2 global reaction mechanism by (Marinov *et al*., 1996) with the 2sCM2 global reaction mechanism in large eddy simulation (LES) modeling of hydrogen enriched methane.

Table 1 : Chemical reaction mechanisms for the oxidation of methane

	Reaction	A	E_a	Order	Equation #
Modified-2sCM2	$CH_4 + 1.5\ O_2 \Rightarrow CO + 2\ H_2O$	2E+15	34500	$[CH_4]^{0.9}[O_2]^{0.5}$	(16)
	$CO + 0.5\ O_2 <=> CO_2$	1E+9	12000	$[CO][O_2]^{0.25}[CO_2]$	(17)

Note: The temperature exponent b is zero in all cases

Table 2 : Global reaction mechanism of hydrogen

	Reaction	A	E_a	Order	Equation #
Hydrogen (Marinov *et al*., 1996)	$H_2 + 0.5\ O_2 \Rightarrow H_2O$	1.8E+16	35002	$[H_2][O_2]^{0.5}$	(18)

Note: The temperature exponent b is zero in all cases, the parent mechanism identities were retained

Computational scheme and solution procedure

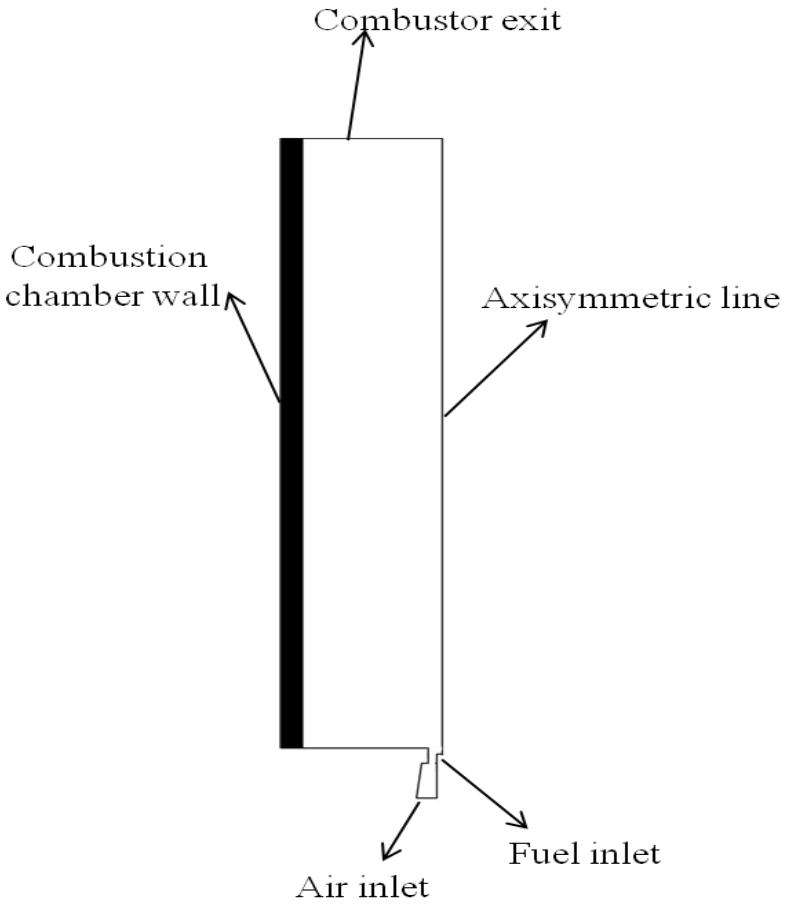

Figure 1: Schematic of the computational domain

A 2-D axisymmetric condition was used to model the combustion in the model gas turbine combustor due to the axial symmetry of the combustor. Additionally, the combustor axis of the flow was parallel to the gravity force. A schematic diagram of the computational geometry of the combustor is shown in Fig.1. The partial differential equations for the conservation of mass, momentum, energy, radiation and species with the appropriate boundary conditions were solved numerically using ANSYS-FLUENT 14 codes. In addition, heat conduction within the combustion chamber wall was also considered. The pressure was discretized using the standard second-order scheme, while other equations were discretized using a second-order upwind scheme. The SIMPLE algorithm was used for pressure-velocity coupling. Further details of the calculation procedure can be found in previous studies (Patankar and Spalding 1972). The solution is said to converge when the maximum residual of the continuity, momentum, turbulent kinetic energy and dissipation rate equations were less than 10^{-4}. The residuals for the energy, radiation and species and NO equations were set to 10^{-6}. The inlet velocity of the fuel and air were supplied depending on the operating conditions of the combustor (fuel energy level, fuel composition and equivalence ratio). The effect of the air swirler was considered by implementing the appropriate axial and tangential velocity boundary conditions. The conjugate heat transfer was solved at the inner wall with a no-slip boundary condition and a no species flux normal to the wall surface applied. The mixed (convection-radiation) heat transfer equation was implemented at the outer wall. A preliminary test was carried out to determine the adequate mesh to model the combustor. Five different mesh sizes were considered as shown in Figure 2. Mesh size of 71,583 cells was observed to give deviation of less than 3% in the temperature profile when compared with that of 86, 899 cells. Therefore a non-uniform grid mesh size of 71,583 was used to model the combustor. To minimize false diffusion errors, more cells were used in the high property gradient region (i.e., vicinity of the wall, inlet and outlet).

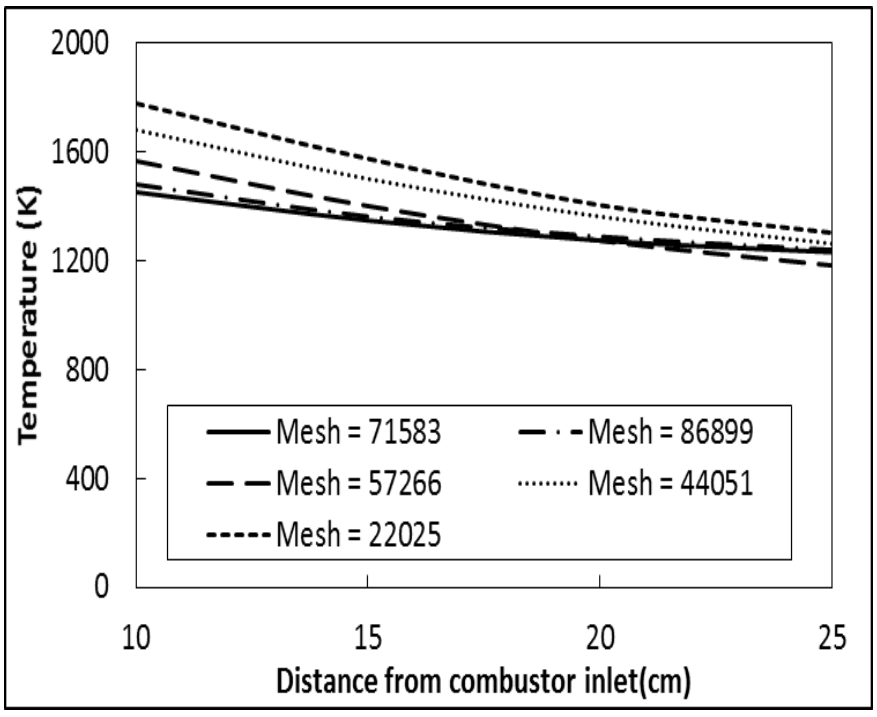

Figure 2: Temperature profile along the combustor axis for different mesh size

Model validation

Experiments were carried out in a non-premixed swirl stabilized combustor at a firing rate of 3.67 MW/m^3 and under ultra-lean conditions (i.e. $\emptyset \leq 0.5$). Details of the set up can be found in (Sanusi *et al*., 2015). The firing rate of 3.67 MW/m^3 fall within the categories of industrial gas turbines that have operating range between 3.5 and 20 MW/m^3-bar (Nemitallah and Habib 2013). The equivalence ratio reported in this work was based on air-fuel ratio such that $\emptyset < 1$ is referred to as lean mixtures. Experimental data were used to validate the numerical model developed as shown in Figures 3 to 5. Figure 3 shows the computed field and images obtained under different operating conditions. The flame shapes are numerically depicted by the temperature contour within the combustor. The highest temperature zone was observed to be from the nozzle exit signifying flame attachment to the nozzle. A high-temperature region was also observed in the outer recirculation zone (ORZ) suggesting the presence of hot combustion products (in the ORZ) as observed in the experiment. Further increase in the equivalence ratio to 0.3 increased the Reynolds number from approximately 12,500 (at Ø=0.5) to approximately 19,000 (at Ø=0.3) based on the burner diameter, thus implying increase in the equivalence ratio enhances the turbulence level in the combustor. The increased turbulence level in the combustor led to the formation of a compact flame near the fuel nozzle. The numerical calculations also captured the flame attachment to the nozzle, with a reduction in the reaction zone that was similarly observed in the experiments. This indicates that the numerical model developed could capture the flame structure at different operating conditions.

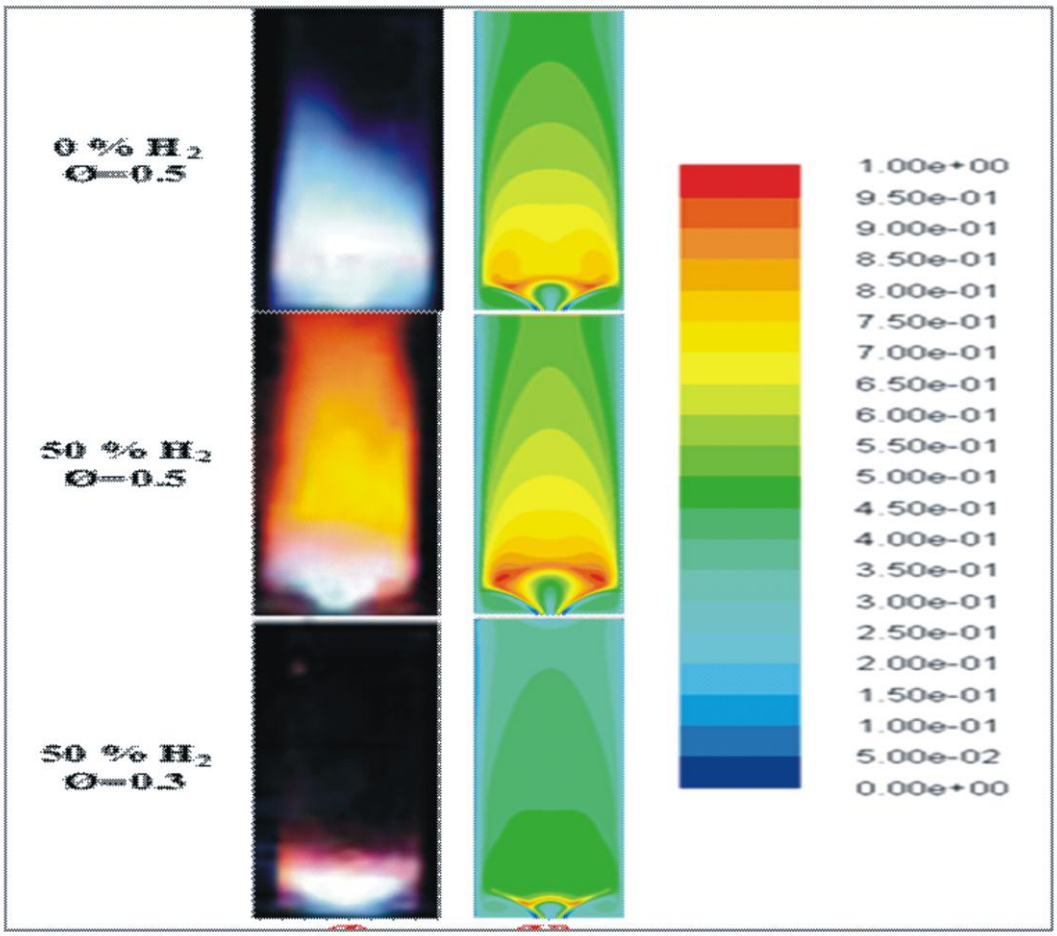

Figure 3: Comparison between the experimental (still picture) and numerical (contours of the temperature) flame shapes at 3.67 MW/m^3

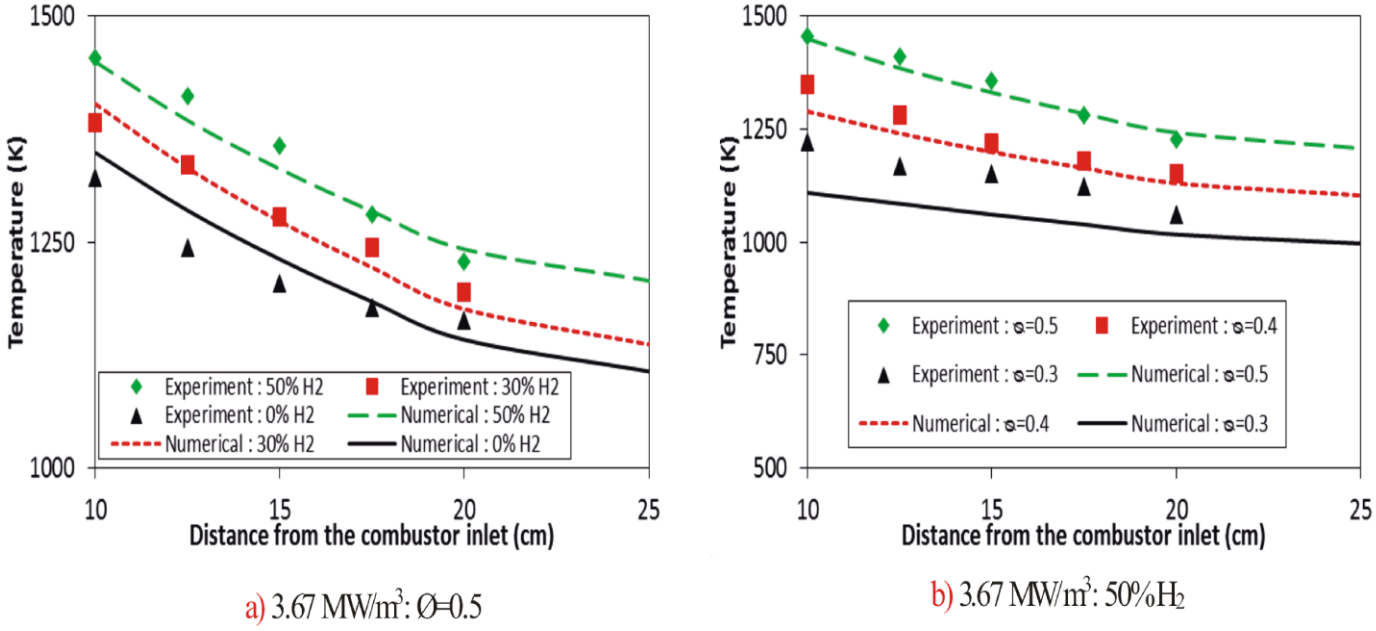

Figure 4: Comparison between the experimental and predicted axial temperature profile

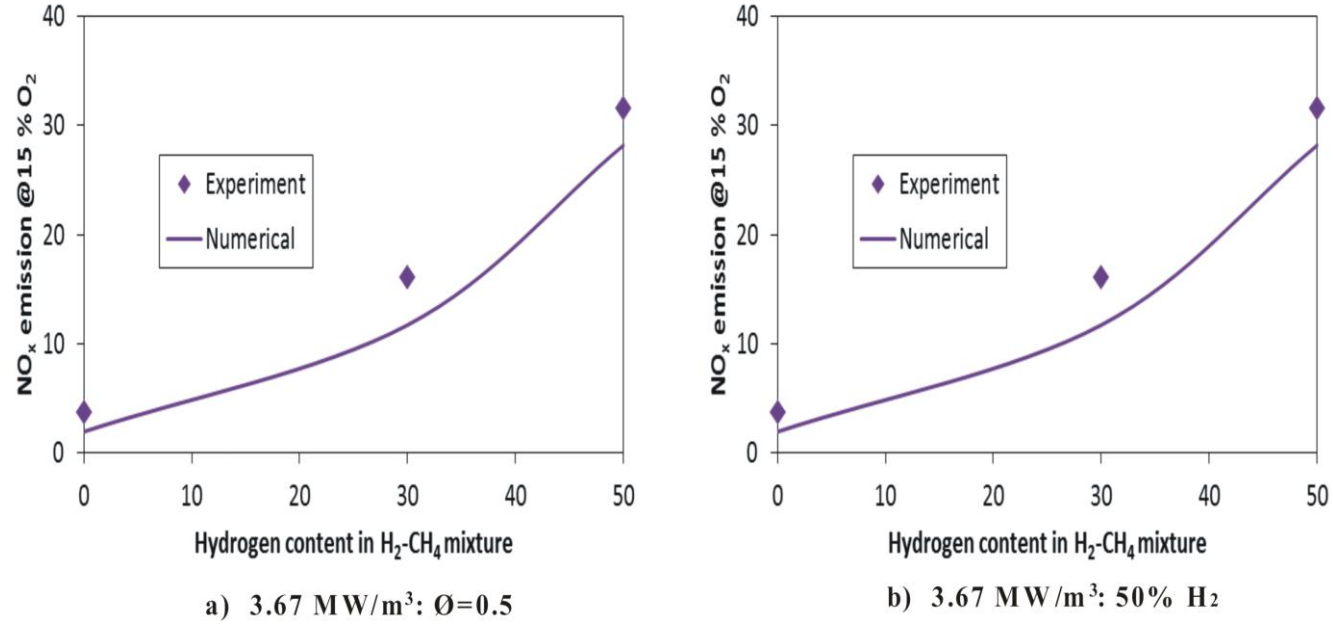

Figure 5: Comparison between the experimental and predicted NOx emission

Figure 4 shows measured and computed temperature profiles along the combustor center line. The combustor temperature generally increases as the hydrogen content in the fuel mixture increases. This increase in temperature is due to higher adiabatic temperature of H_2 compared to that of methane. At 50% H_2 and Ø =0.3 (see Figure 4b), the model presented under-predicts the temperature profile in the combustor. However, the predicted temperature profile was within 10% of the experimental values.

The NOx emissions from the combustor depend on some competing factors such as the combustor temperature, the oxygen availability and the residence time of the combustion product. Measured and the predicted NOx emissions are shown in Figure 5. The figure shows that increasing the equivalence ratio and hydrogen contents in the CH_4-H_2 mixture increases the NOx emissions. This increase can be attributed to the increase in the adiabatic temperature at these conditions. This trend was observed experimentally and through numerical calculations in this study. The combustor maximum temperature was observed to have significant effect on the amount of NOx emissions. Thus, accurate prediction of the combustor maximum temperature is critical to an accurate NOx prediction. The Modified-2sCM2 mechanism presented in this paper was observed to be consistent with the prediction of the combustor temperature, major species and the NOx emissions with a reasonable degree of accuracy.

RESULTS AND DISCUSSION

Effect of swirl number on combustor flow field

Figure 6 shows the stream line of the flow pattern on the computed heat of reaction and temperature contour in order to study the effect of swirl number on the flow pattern. Three different recirculation zone patterns were generally observed: the outer recirculation zone [ORZ], the inner recirculation zone [IRZ] and the wake recirculation zone [WRZ]. The ORZ are generally formed due to the sudden expansion at the dump plane of the combustor, the IRZ are formed due the vortex break down of the flow while the WRZ are formed around the bluff body inserted into the fuel pipe. The contour of the heat of reactions shows that the flames are anchored at the inner shear layer of the flow (between the jet flow and the IRZ) and terminate at the onset of the IRZ. The disappearance of the active reaction zone is due to the vortex rolled up of the flame. The vortex rolled up results in the recirculation of high temperature combustion product that preheats the incoming fresh charge to the combustor, thus, stabilizing the flame. As the SN increased, the recirculation region becomes wider enabling the IRZ to move towards the combustor inlet, thus, leading to a more compact flame. Also, the size of the WRZ increased as the SN increased due to the reduced axial component of the velocity. The increased size of the WRZ forces the IRZ to shift towards the combustor wall leading to an increase in the flame angle. Furthermore it gives room for the IRZ to approach the combustor inlet, thus, allowing the early attainment of the ignition temperature by the fresh charges. The temperature contour (Figure 6b) shows that the hot combustion product in the eye of the IRZ plays an important role in preheating the incoming charges and flame stabilization. The local hotspot in the flame was observed to decrease at higher SN. This was due to improved mixing and turbulence at higher SN. The temperature contour further shows that downstream of the IRZ, the combustion is near completion, such that the heat transfers downstream of the flame is due to heat exchange between the combustion products and wall of the combustor. In order to quantify the IRZ, the axial velocity along the combustor axis was plotted as shown in Figure. 7. An inset of the expanded view of the recirculation region is given in each figure. The IRZ in the combustor serves as aerodynamic blockage resulting in the acceleration the flow at the combustor inlet. Hence, higher axial velocities were generally observed at the combustor inlet. Higher axial velocity at SN of 0.38 was also observed at all operating conditions. Cases with SN of 0.67 were found to be optimum based on the fact that the highest size and strength of the recirculation zone is observed at these conditions.

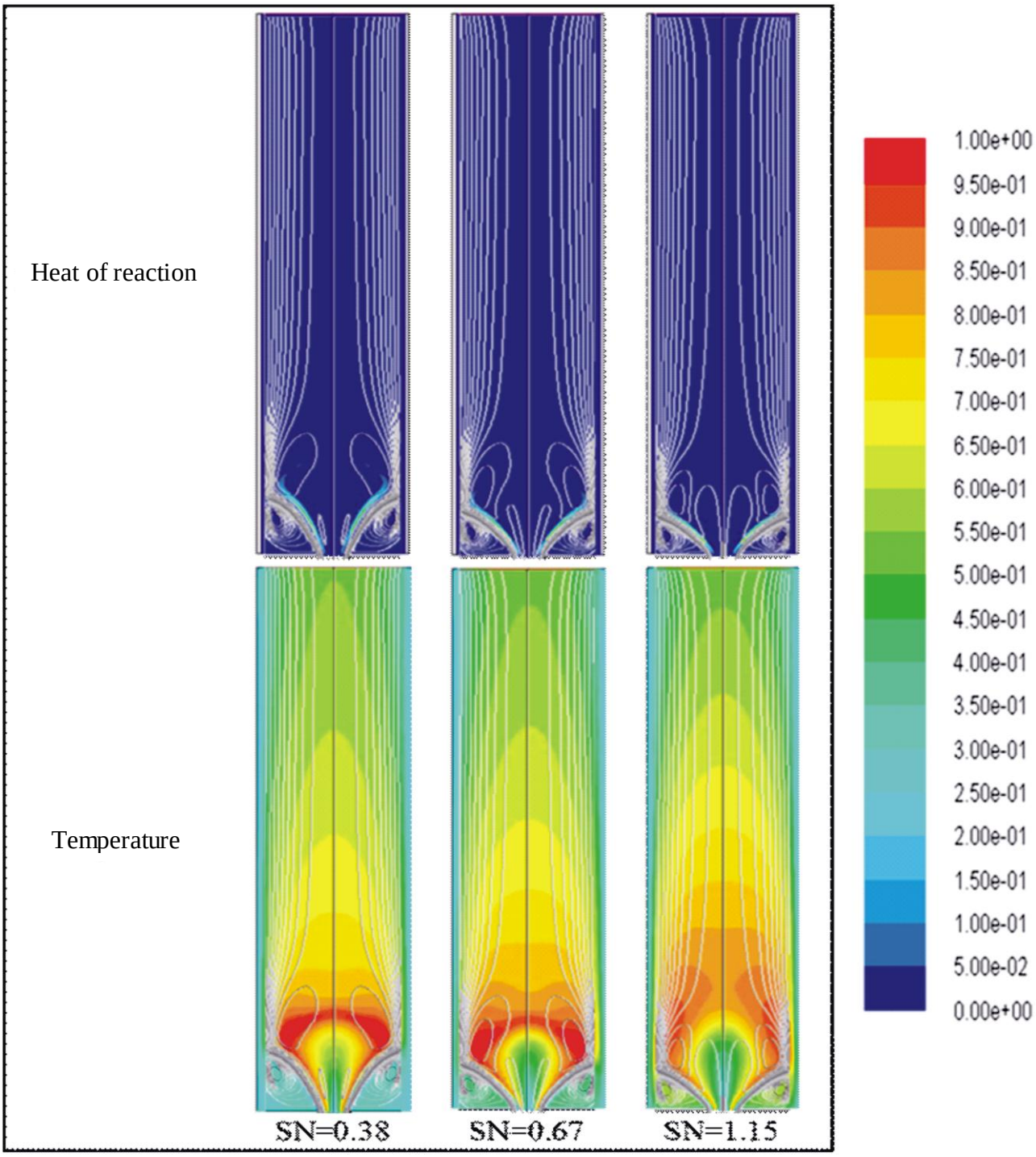

Figure 6: The computed heat of reaction and temperature contour of different

SN for 50% H_2: Ø = 0.5

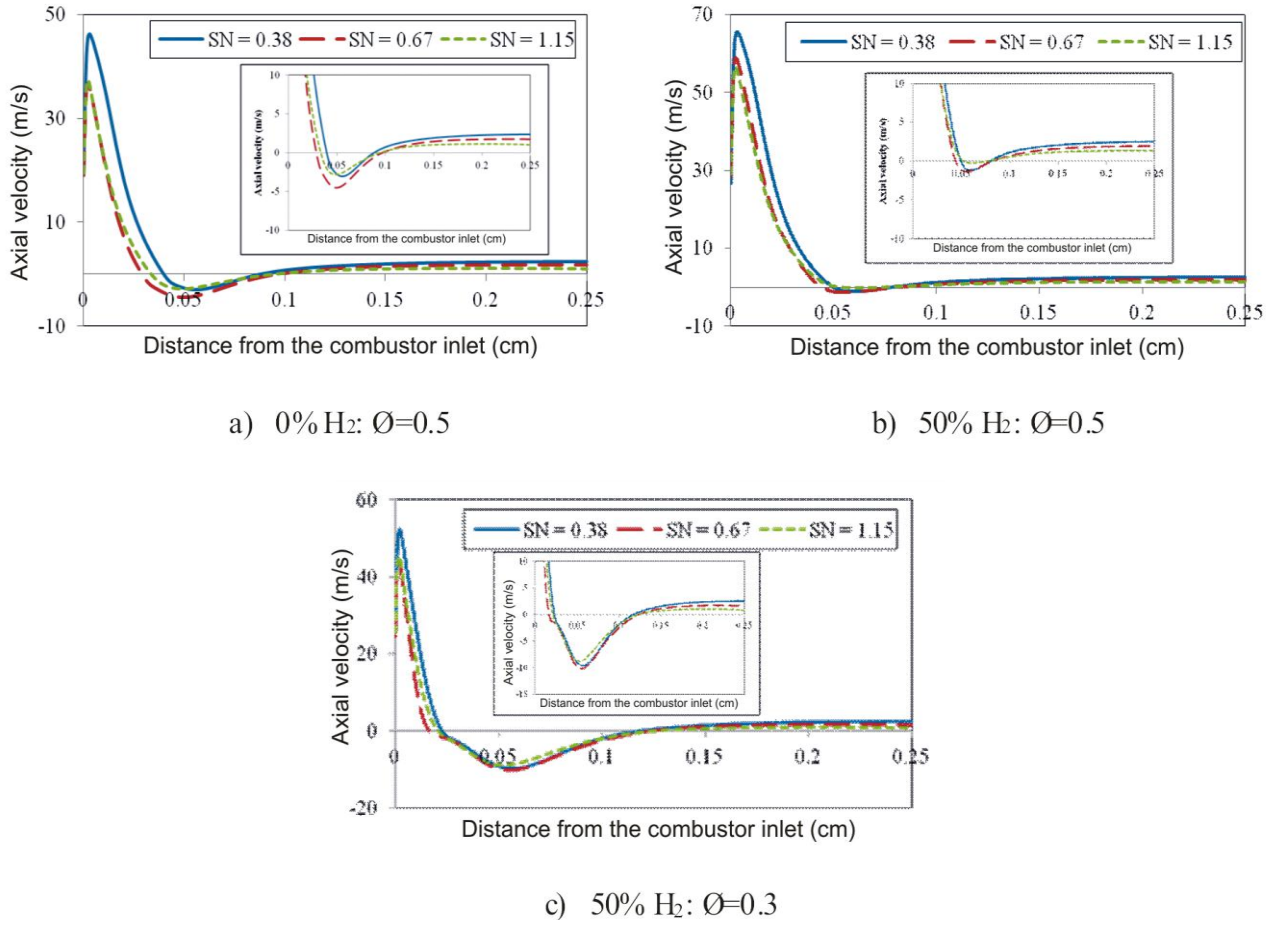

Figure 7: Effect of swirl number on the axial velocity profile along the combustor axis under different operating conditions

Effect of swirl number on combustor temperature profile

Figure 8 shows the temperature profile along the combustion center downstream of the flame. A larger recirculation zone comprising of both the IRZ and WRZ led to the increased level of turbulence and amount of hot gas re-circulated. It also increased the combustion residence time. A more compact flame was observed at this condition, which implies the propensity of high heat release and flame temperature within the zones. The heat transfers downstream of the RZ were generally due to heat loss from the combustion product to the wall and the excess air supplied. At 0% H_2 and SN=0.38 (Figure 8a), the flame became less compact and the reaction and heat release continues as the exhaust gas approaches the combustor exit leading to higher temperature at the combustor exit as compared to the case of SN=1.15. While for higher SN cases, the temperature is essentially due to heat loss from the combustion product to combustor wall and excess air. For cases with hydrogen in the fuel mixtures, higher temperature was observed as the SN increased (Figure 8b and Figure 8c). For a case of 50% H_2: Ø=0.5 (Figure 3), where UHCs are observed in the combustor. Increasing the SN can be a means of improving the combustion efficiency due to increased residence time and turbulence. Thus, more of the fuel that hitherto goes unburned is combusted and release more heat energy leading to increased combustion temperature.

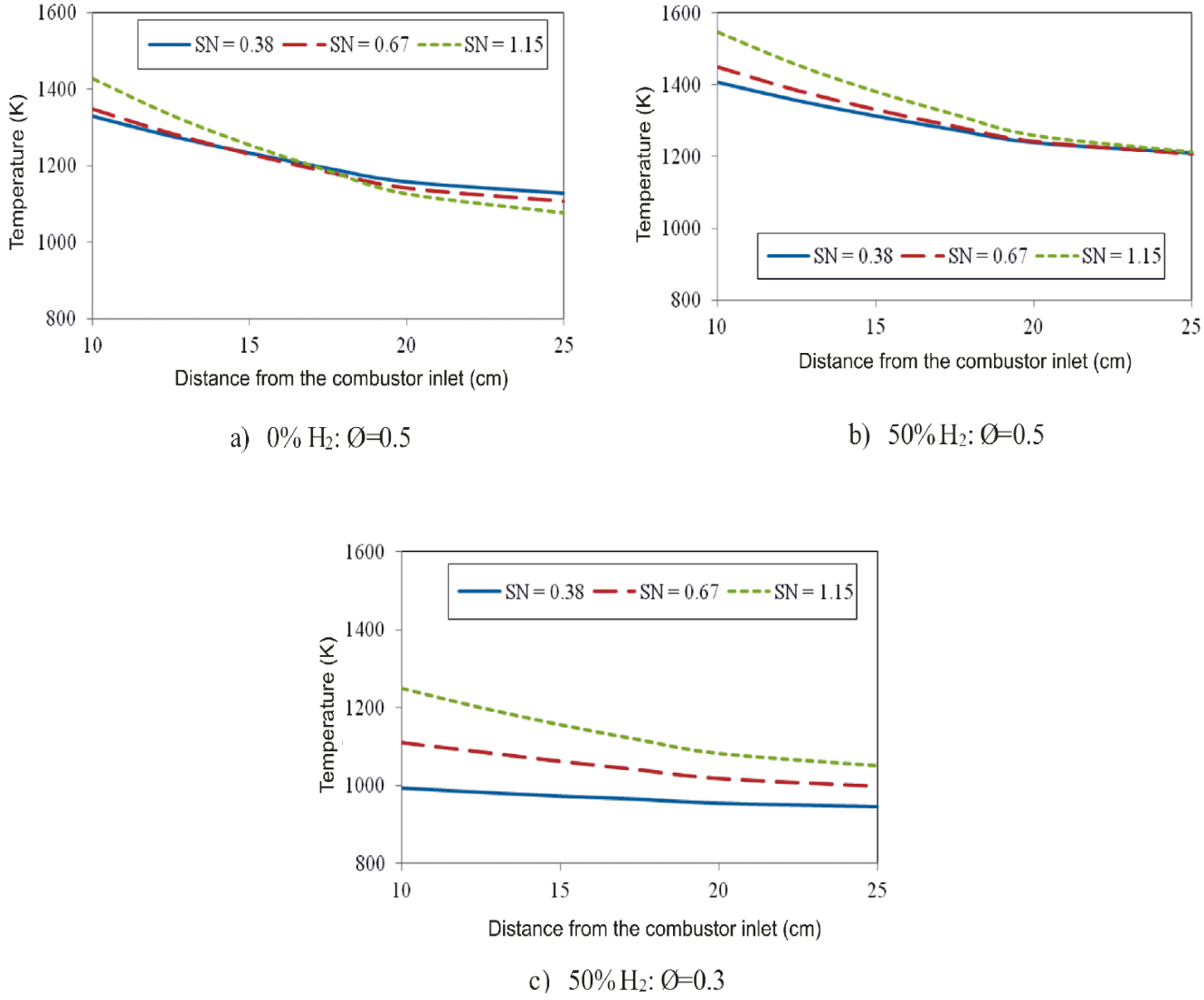

Figure 8: Effect of swirl number on the temperature profile along the combustor axis under different operating conditions

Effect of swirl number on combustor emission

The effects of SN on the emission at different operating conditions are summarized in Figure 9. For 0% H_2, the SN of up to 0.67 produced near zero CO emission. Further increase in the SN, however, drastically increase the CO emission. The CO emission at this condition is 10,463 ppm (not shown on the graph). This high CO can be attributed to higher turbulence observed at SN = 1.15, leading to local flame extinction. Similar trend was observed for the case of 50% H_2: Ø = 0.5, the CO emission at this condition is higher than the case of 0% H_2. This is attributed to the inhibition of the methane oxidation and reduced IRZ. An increase in the SN continuously decrease the CO emissions for the case of 50% H_2, Ø=0.3. At this operating conditions (Re = ~19,500), the CO is solely dependent on the residence time of the combustion product. Thus, an increase in the SN increased the residence time. The increased residence time enable the complete burnout of CO to CO_2. The increased SN also increases the turbulence mixing, thus, reducing the local hotspot in the combustor. Figure 9b shows that the NOx emission decreased with increasing SN. This was expected since the combustion maximum temperature similarly decreased with SN.

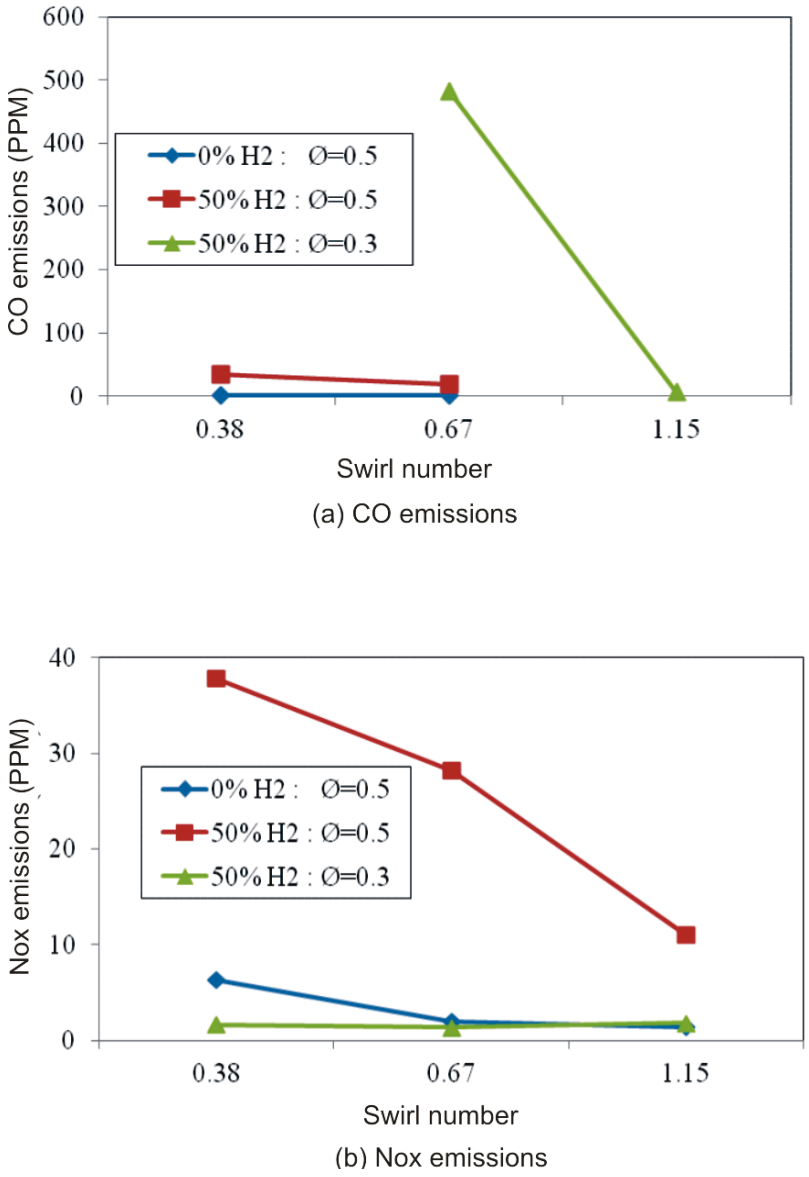

Figure 9: Effect of swirl number on the combustor emissions under different operating conditions

CONCLUSIONS

The effect of swirl number on the combustion characteristics and emission in a gas turbine model combustor has been numerically studied and the following conclusions were drawn.

The local hotspot in the flame was observed to decrease as the swirl number (SN) increased due to improved mixing and turbulence in the combustor.

Flames with SN of 0.67 were found to be optimum. This was due the fact that the highest size and strength of the recirculation zone that enhance flame stabilization are observed at SN of 0.67.

The combustor exit temperature decreased with increasing SN.

For case of pure methane combustion (0% H_2), the CO emission initially decreased when the swirl number increased from 0.38 to 0.67 and thereafter increased. The initial decrease of CO emission can be attributed to improved mixing and turbulence in the combustor that aided the complete combustion of CO to CO_2. The later increase in the CO emission was due to a more vigorous mixing that results in the local quenching of the flame.

The NOx emission decreased with increasing SN at all operating conditions. This was due to the decreased combustion maximum temperature as the SN increases.

Nomenclature

A	Pre-exponential factor	$\hat{P}_i$	Pressure magnitude (N/m^2)
b	Temperature exponent	R_j	species equation source term (kg/m^3s)
CO	Carbon monoxide	$S_\emptyset$	energy source term (W/m^3)
CO_2	Carbon dioxide	SN	Swirl number
CH_4	Methane	t_{ij}	Viscous stress tensor (N/m^2)
$D_{j,m}$	diffusion flux of specie j (m^2/s)	T	Temperature (K)
E_a	Activation energy (kJ/kmolK)	T_w	Wall temperature (T)
H_2	Hydrogen gas	T_a	ambient temperature (T)
k	Turbulent kinetic energy (m^2/s^2)	u_i	Fluid velocity component in the x_i (m/s)
K_r	Rate constant (m^3/s)	x	Distance (m)
k_q	Thermal conductivity (W/mK)	Y_j	Mass fraction of specie j
NOx	Nitrogen oxide		
	Greek symbols		
ϵ	emissivity	μ	dynamic viscosity (Ns/m^2)
ρ	Density (kg/m^3)	μ_t	turbulent viscosity (Ns/m^2)
Ø	Equivalence ratio	∩	characteristics swirl number
ε	Turbulent dissipation rate (m^2/s^3)	α_s	swirl constant

REFERENCES

De, A., and Acharya, S. (2012). Parametric study of upstream flame propagation in hydrogen-enriched premixed combustion: Effects of swirl, geometry and premixedness. *International Journal of Hydrogen Energy* 37 (19):14649-14668.

Ghenai, C. (2010). Combustion of Syngas Fuel in Gas Turbine Can Combustor. *Advances in Mechanical Engineering* 2010.

Habib, M. A., Ben-Mansour, R., Badr, H. M., Ahmed, S. F. and Ghoniem A. F. Computational fluid dynamic simulation of oxyfuel combustion in gas-fired water tube boilers. *Computers and Fluids* 56:152-165.

Habib, M. A., Mokheimer, E. M., Sanusi, S. Y. and Nemitallah, M. A. (2014). Numerical investigations of combustion and emissions of syngas as compared to methane in a 200 MW package boiler. *Energy Conversion and Management* 83:296-305.

Li, G.-n., H. Zhou, and K.-f. Cen. (2008). Emission characteristics and combustion instabilities in an oxy-fuel swirl-stabilized combustor. *Journal of Zhejiang University-SCIENCE A* 9 (11):1582-1589.

Liu, J., Z. Liu, S. Chen, S. O. Santos, and Zheng C. (2017). A numerical investigation on flame stability of oxy-coal combustion: Effects of blockage ratio, swirl number, recycle ratio and partial pressure ratio of oxygen. *International Journal of Greenhouse Gas Control* 57:63-72.

Marinov, N., Wcstbrook, C. and Pitz W. (1996). DETAILED AND GLOBAL CHEMICAL KINETICS MODEL FOR. *Transport phenomena in combustion* 1:118.

Mokheimer, E., Sanusi, Y. S. and Habib, M. A. (2015). Numerical study of hydrogen-enriched methane–air combustion under ultra-lean conditions. *International Journal of Energy Research*.

Nemitallah, M. A., and M. A. Habib. Experimental and numerical investigations of an atmospheric diffusion oxy-combustion flame in a gas turbine model combustor. *Applied Energy* 111:401-415.

Nemitallah, M. A. and Habib, M. A. (2013). Experimental and numerical investigations of an atmospheric diffusion oxy-combustion flame in a gas turbine model combustor. *Applied Energy* 111:401-415.

Patankar, S. V., and Spalding, D. B. (1972). A calculation procedure for heat, mass and momentum transfer in three-dimensional parabolic flows. *International Journal of Heat and Mass Transfer* 15 (10):1787-1806.

Reynolds, W. C. (1987). Fundamentals of turbulence for turbulence modeling and simulation. *Lecture Notes for Von Karman Institute, Agard Report No. 755*.

Sanusi, Y. S., Habib, M. A. and Mokheimer, E. M. (2015). Experimental study on the effect of hydrogen enrichment of methane on the stability and emission of nonpremixed swirl stabilized combustor. *Journal of Energy Resources Technology* 137 (3):032203.

Sanusi, Y. S., Mokheimer, E. M., Shakeel, M. R., Abubakar, Z.and Habib, M. A. (2017). Oxy-Combustion of Hydrogen-Enriched Methane: Experimental Measurements and Analysis. *Energy and Fuels* 31 (2):2007-2016.

Seebold, J., J. Bloomquist, and Christy, R. (2001). Gas Turbine NOx Reduction Retrofit. Paper read at SPE/EPA/DOE Exploration and Production Environmental Conference.

Shanbhogue, S., Sanusi, Y., Taamallah, S., Habib, M., Mokheimer, E. and Ghoniem, A. (2016). Flame macrostructures, combustion instability and extinction strain scaling in swirl-stabilized premixed CH 4/H 2 combustion. *Combustion and Flame* 163:494-507.

Shih, T.-H., Liou, W. W., Shabbir, A., Yang, Z. and Zhu, J. (1995). A new k-*e* eddy viscosity model for high reynolds number turbulent flows. *Computers and Fluids* 24 (3):227-238.

Smith, L. M., and Woodruff, S. L. (1998). Renormalization-group analysis of turbulence. *Annual Review of Fluid Mechanics* 30 (1):275-310.

USEPA. (2015). United State Environmental Protection Agency Retains the Primary National Ambient Air Quality Standards for Oxides of Nitrogen.https://www.cfrenvironmental.com/single-post/2018/04/24/USEPA-Retains-the-Primary-National-Ambient-Air-Quality-Standards-for-Oxides-of-Nitrogen.

USEPA. (2018). Alternative Control Techniques Document-NOx Emissions from Stationary Gas Turbines. United State Environmental Protection Agency. https://www3.epa.gov/ttncatc1/dir1/gasturb.pdf.

Weigand, P., Meier, W., Duan, X. R., Stricker, W. and Aigner, M. (2006). Investigations of swirl flames in a gas turbine model combustor: I. Flow field, structures, temperature, and species distributions. *Combustion and Flame* 144 (1-2):205-224.

Yakhot, V., and Orszag, S. A. (1986). Renormalization group analysis of turbulence. I. Basic theory. *Journal of scientific computing* 1 (1):3-51.

Zheng, Y., J. Fan, Y. Ma, P. Sun, and K. Cen. (2000). Computational modeling of tangentially fired boiler(II) NOx emissions. *Chinese Journal of Chemical Engineering* 8 (3):247-250.